# Spatiotemporal patterns of tree growth as related to carbon isotope fractionation in European forests under changing climate

**Running head:** Ecophysiology of forest growth in Europe

Tatiana A. Shestakova[1,2], Jordi Voltas[2], Matthias Saurer[3], Frank Berninger[4], Jan Esper[5], Laia Andreu-Hayles[6], Valérie Daux[7], Gerhard Helle[8], Markus Leuenberger[9], Neil J. Loader[10], Valérie Masson-Delmotte[7], Antonio Saracino[11], John S. Waterhouse[12], Gerhard H. Schleser[13], Zdzisław Bednarz[14], Tatjana Boettger[15], Isabel Dorado-Liñán[16], Marc Filot[9†], David Frank[17], Michael Grabner[18], Marika Haupt[15], Emmi Hilasvuori[19], Högne Jungner[19], Maarit Kalela-Brundin[20], Marek Krąpiec[21], Hamid Marah[22], Sławomira Pawełczyk[23], Anna Pazdur[23], Monique Pierre[7], Octavi Planells[24], Rūtilė Pukienė[25], Christina E. Reynolds-Henne[26], Katja T. Rinne[27], Angelo Rita[28], Eloni Sonninen[19], Michel Stiévenard[7], Vincent R. Switsur[12‡], Elżbieta Szychowska-Krąpiec[21], Malgorzata Szymaszek[23§], Luigi Todaro[28], Kerstin Treydte[3], Adomas Vitas[29], Martin Weigl[30], Rupert Wimmer[31], Emilia Gutiérrez[24*]

[1] Woods Hole Research Center, Falmouth, MA, USA

[2] Department of Crop and Forest Sciences – AGROTECNIO Center, University of Lleida, Lleida, Spain

[3] Swiss Federal Research Institute WSL, Birmensdorf, Switzerland

[4] Department of Forest Sciences, University of Helsinki, Helsinki, Finland

[5] Department of Geography, Johannes Gutenberg University, Mainz, Germany

[6] Tree-Ring Laboratory, Lamont-Doherty Earth Observatory of Columbia University, Palisades, USA

[7] Laboratory for Climate and Environmental Sciences, CEA/CNRS/UVSQ, Gif-sur-Yvette, France

[8] Helmholtz-Centre Potsdam, German Centre for Geosciences – GFZ, Potsdam, Germany

[9] Climate and Environmental Physics, University of Bern, Bern, Switzerland

[10] Department of Geography, Swansea University, Swansea, UK

[11] Department of Agricultural Sciences, University of Naples Federico II, Portici, Italy

[12] Department of Biomedical and Forensic Sciences, Anglia Ruskin University, Cambridge, UK

[13] FZJ Research Center Jülich, Institute of Bio- and Geosciences IBG-3, Jülich, Germany

[14] Department of Forest Biodiversity, Agricultural University, Krakow, Poland

[15] Department of Isotope Hydrology, Helmholtz Centre for Environmental Research – UFZ, Halle, Germany
[16] Forest Research Centre, National Institute for Agricultural Research and Experimentation (INIA-CIFOR), Madrid, Spain
[17] Laboratory of Tree-Ring Research, University of Arizona, Tucson, USA
[18] Institute of Wood Technology and Renewable Resources, University of Natural Resources and Life Sciences – BOKU, Vienna, Austria
[19] Laboratory of Chronology, University of Helsinki, Helsinki, Finland
[20] Forestry Museum, Lycksele, Sweden
[21] Faculty of Geology, Geophysics and Environmental Protection, AGH University of Science and Technology, Krakow, Poland
[22] Water and Climate Unit, CNESTEN, Rabat, Morocco
[23] Department of Radioisotopes, Silesian University of Technology, Gliwice, Poland
[24] Department of Biological Evolution, Ecology and Environmental Sciences, University of Barcelona, Barcelona, Spain
[25] Nature Research Centre, Institute of Geology and Geography, Vilnius, Lithuania
[26] Oeschger Centre for Climate Change Research, University of Bern, Bern, Switzerland
[27] Natural Resources Institute Finland (Luke), Vantaa, Finland
[28] School of Agricultural, Forest, Food and Environmental Sciences, University of Basilicata, Potenza, Italy
[29] Environmental Research Centre, Vytautas Magnus University, Kaunas, Lithuania
[30] Holzforschung Austria, Vienna, Austria
[31] Institute for Natural Materials Technology, University of Natural Resources and Life Sciences, Tulln, Austria
[†] Present address: CSL Behring AG, Bern, Switzerland
[‡] Deceased
[§] Present address: Janusz Kusocinski Sports School in Zabrze, Zabrze, Poland

[*]Corresponding author: Emilia Gutiérrez
Tel: +34 934037143
Email: emgutierrez@ub.edu

**Acknowledgements**

T.A.S. acknowledges the ERANET-Mundus program (European Commission, Grant agreement 20112573), the COST Action FP1304 via the STSM program (European Commission, COST-STSM-ECOST-STSM-FP1304-140915-066395), and the Spanish Government (grant number AGL2015-68274-C3-3-R). This study was supported by the EU-project ISONET (EVK2-2001-00237). We are also grateful to Carmela Miriam D'Alessandro, Nathalie Etien, Marie-Thérèse Guillemin and Werner Laumer for field and laboratory assistance.

**Abstract**

*Aim*

To decipher continent-wide spatiotemporal patterns of forest growth dynamics and their associations with carbon isotope fractionation processes inferred from tree rings as modulated by climate warming in Europe.

*Location*

Europe and North Africa (30–70°N, 10°W–35°E).

*Time period*

1901–2003.

*Major taxa studied*

Temperate and Euro-Siberian trees.

*Methods*

We characterize changes in the relationship between tree productivity and carbon isotope fractionation over the 20$^{th}$ century using a European network. Using indexed tree-ring widths ($TRW_i$), we assess shifts in the temporal coherence of radial growth (synchrony) for five forest ecosystems (Atlantic, Boreal, cold continental, Mediterranean and temperate). We also examine whether $TRW_i$ shows increased coupling with leaf-level gas exchange, inferred from indexed carbon isotope discrimination in tree-ring cellulose ($\Delta^{13}C_i$), through enhanced stomatal regulation in response to amplified drought stress spreading northwards.

*Results*

We find spatial autocorrelation for $TRW_i$ and $\Delta^{13}C_i$ extending over up to 1,000 km among forest stands. However, growth synchrony is not uniform across Europe, but increases along a latitudinal gradient concurrent with decreasing temperature and evapotranspiration. Latitudinally-structured relationships between $TRW_i$ and $\Delta^{13}C_i$ (changing from negative to positive as latitude increased) point to drought impairing carbon uptake via stomatal regulation of water losses as the main mechanism underlying synchronous forest growth in continental Europe below 50°N. At the turn of this century, warming-induced effects on leaf physiology increased synchrony in tree growth among European forests to unprecedented levels over the last century.

*Main conclusions*

Increased growth synchrony from the first to the second half of the 20$^{th}$ century in Mediterranean, temperate and cold continental forests, together with a tighter relationship between $TRW_i$ and $\Delta^{13}C_i$, indicate increasing drought effects on productivity across Europe. Such recent tendency towards exacerbated moisture-sensitive forest growth could override a positive effect of enhanced leaf intercellular $CO_2$ concentration, resulting in forthcoming declines in forest carbon gain continent-wide.

**Keywords:** carbon isotopes, climate change, dendroecology, drought stress, European forests, latitudinal gradients, *Pinus*, *Quercus*, stomatal control, tree rings

## Introduction

Understanding the physiological mechanisms underlying variations in forest productivity is a key priority in global change research. Factors such as tree age, forest structure and management, nutrient availability, pollution and disturbance regimes influence the carbon budget of forested areas. During the last decades, however, climate change and increased atmospheric $CO_2$ ($_{atm}CO_2$) have largely altered the growth of natural forests (Nabuurs et al., 2013). To explore these dynamics, research efforts have been mainly confined to local ecosystems, with some representative woody species and their interactions examined at small spatial scales (Pivovaroff et al., 2016). This approach is hampered by site-dependent effects and limited representativeness of environmental conditions. A comprehensive understanding of tree functioning is urgently needed across broad regions in order to assess the potential and limits of forest carbon uptake globally (Chown, Gaston, & Robinson, 2004). Through the analysis of meaningful functional traits (Violle, Reich, Pacala, Enquist, & Kattge, 2014), the interpretation of spatiotemporal patterns of forest growth variability can provide comprehensive insights into the environmental responses that may change forest's services for carbon storage in the next decades (Anderegg et al., 2016).

The mechanisms and processes influencing forest productivity are extremely variable (Gibert, Gray, Westoby, Wright, & Falster, 2016). Despite such complexity, regionally coherent multispecies responses have been linked to global change effects on forest ecosystems using tree-ring networks (Babst et al., 2013; Shestakova et al., 2016). Dendroecological studies rely on the presence of common signals archived in tree populations, which are often derived from ring-width series reflecting variations in environmental factors (Fritts, 2001). Alternatively, stable isotopes are proxies of ecophysiological traits that are valuable to assess plant carbon and water relations at large spatiotemporal scales (Werner et al., 2012; Frank et al., 2015). In particular, the carbon isotope discrimination ($\Delta^{13}C$) of tree rings reflect more directly the complex array of physiological responses to environmental conditions than classical dendrochronological traits such as ring-width (Treydte et al., 2007; Gessler et al., 2014). The ratio of the heavy to light carbon isotopes ($^{13}C/^{12}C$) of organic matter depends on factors affecting $CO_2$ assimilation, which is mainly controlled by photosynthetic rate ($A$) and stomatal conductance ($g_s$) (Farquhar, Ehleringer, & Hubick 1989). Hence, the interannual variation in $\Delta^{13}C$ can be evaluated and retrospectively related to leaf-level physiological processes (e.g., Andreu-Hayles et al., 2011; Shestakova, Aguilera, Ferrio, Gutiérrez, & Voltas, 2014). This is especially relevant in temperate forests thriving under near-optimal conditions, where tree growth patterns may not be informative of climate variability, but stable isotopes have been

shown to be sensitive to environmental variables (Hartl-Meier et al., 2015). Indeed, much complementary information can be gained by analysing carbon isotopes in addition to ring-widths (Cernusak & English, 2015), which together provide relevant evidence on how trees respond to climate change and increasing $_{atm}CO_2$ (Andreu-Hayles et al., 2011; Saurer et al., 2014).

In drought-prone environments, tree-ring $\Delta^{13}C$ can be mainly related to the stomatal control of $CO_2$ fluxes into the leaf, integrating any environmental variable affecting stomatal conductance (Gessler et al., 2014). Under such conditions, radial growth and $\Delta^{13}C$ are bound together by two factors: stomatal regulation and water availability. However, $\Delta^{13}C$ is also affected by changes in photosynthetic activity associated with irradiance, phenology, nutritional stresses or N deposition when water becomes less limiting (Livingston et al., 1998). By combining ring-width and $\Delta^{13}C$, information can be gained on the array of tree performances that underlie biogeographical interactions, as these traits share spatial responses to drought events (Voelker, Meinzer, Lachenbruch, Brooks, & Guyette, 2014).

In the present study, we attempt to characterize the degree of dependence of stem growth on photosynthetic carbon isotope fractionation across European forests using a unique tree-ring network (Treydte et al., 2007). So far, only the isotope data of this network have been analysed, but not radial growth, nor the relationship between the two parameters. We used 20 chronologies from old trees comprising conifers (*Pinus*) and oaks (*Quercus*) spanning the 20$^{th}$ century and ranging from Mediterranean to Boreal latitudes (37°N to 69°N). Indeed, latitudinal gradients are extremely relevant for the analysis of large-scale patterns of trait variability and their relationships with ecosystem functioning (Violle et al., 2014). We hypothesise that, on a continental scale, (*i*) the temporal coherence of radial growth in forest trees is geographically structured, with more synchronous growth to be found among cold-limited, high latitude forests than among drought-prone, low-latitude forests (Shestakova et al., 2016); (*ii*) these patterns of synchrony are linked to the relative significance of carbon assimilation and stomatal control on growth determination, as reflected by relationships between ring-widths and $\Delta^{13}C$; and (*iii*) warming-induced drought stress triggers a tighter stomatal control of water losses which, in turn, enhances synchrony in low latitude forests owing to more coordinated physiological reactions to climate. On the basis of the joint analysis of radial growth and $\Delta^{13}C$, the assessment of spatiotemporal tree responses to environmental changes may improve our understanding of growth and physiology changes experienced by European forests throughout the 20$^{th}$ century.

## Materials and methods

*Tree-ring network*

We used a tree-ring dataset from the pan-European network ISONET (European Union, EVK2-2001-00237), which is comprised of 20 sites and provides a comprehensive coverage of the biogeographic conditions that are found across Europe into northern Africa (Treydte et al., 2007) (Table 1). Sites consist of old-grown forests (mean age = 454 ± 196 years [SD]) from the two main genera in Europe (*Pinus* and *Quercus*) plus *Cedrus atlantica* (Morocco). The forests originate from semiarid (Mediterranean basin), humid temperate (western-central Europe), cold continental (north-central Europe) and subarctic (Fennoscandia) climates (Table 1). The sampled trees are temperate (*Quercus petraea, Q. robur*) and Euro-Siberian (*Pinus nigra, P. sylvestris, P. uncinata*) taxa, with sites distributed across most of their climatic ranges (Table 1). Sampled stands spread along broad latitudinal (from 32°58'N to 68°56'N) and altitudinal (from 5 m to 2,100 m a.s.l.) gradients, with high-elevation sites concentrated in southern Europe. Conifers are the dominant species in unmanaged cold Boreal or Mediterranean zones (i.e., high-latitude or high-elevation sites), whereas oaks are mainly found in humid western and central European lowlands. The distance between sites varies from about 50 km up to 4,500 km.

Increment cores were extracted from numerous trees at each site (Table S1), and tree rings were cross-dated and measured following standard dendrochronological procedures (Cook & Kairiukstis, 1990). As a proxy for above-ground woody biomass accumulation, basal area increment (BAI) for each stand was calculated as the bi-weight site mean of BAI of individual ring-width series. Temporal trends in the BAI chronologies were estimated through the slope (*b*) of the linear regression of BAI records on time. Indexed tree-ring width ($TRW_i$) and carbon isotope discrimination ($\Delta^{13}C_i$) chronologies were obtained by high-pass filtering and autocorrelation removal (see Appendix 1 in Supporting Information). Details on tree-ring network characteristics can be found in Appendix 2. The indexed ring-width and isotope chronologies were used as input for statistical analyses. The study period was 1901–2003.

*Analysis of spatial variability of tree growth*

Spatial structure of tree-ring traits and climatic signals across Europe

The temporal coherence of tree-ring signals ($TRW_i$, $\Delta^{13}C_i$) among sites was characterized to determine how far such coherence extends over Europe. To this end, correlation coefficients (*r*) between pairs of chronologies, calculated over the period 1901–2003, were regressed on their geographic distance using a negative exponential function for both $TRW_i$ and $\Delta^{13}C_i$. The modified correlogram technique (Koenig & Knops, 1998) was also employed to characterize

the spatial autocorrelations in the network. To this end, the statistical significance of the pairwise correlations among chronologies was calculated within classes located 500 km apart. Chronologies located farther than 2,500 km apart were combined into a single class. Hence, six classes were defined ranging from <500 to >2,500 km. To evaluate the geographic extent of synchrony in climate factors, the same analysis was performed for mean annual temperature and precipitation.

Temporal coherence of ring-width signals

The investigation of common $TRW_i$ variability among chronologies (growth synchrony, $\hat{a}$) was performed through variance-covariance (VCOV) modelling following Shestakova et al. (2014, 2018) (Appendix 3.1). This approach is suited to test the presence of contrasting tree-ring patterns in pre-established groups of chronologies, where particular groups can be defined based on existing knowledge (Shestakova et al., 2018). Here, the 20 chronologies were classified into four groups according to membership to a particular climate type following the Köppen climate classification (Köppen & Geiger, 1936): Boreal (*Dfc*), cold continental (*Dfb*), humid temperate (C*fb*) and Mediterranean (*Csb*) (Table 1). In turn, the humid temperate climate was split into Atlantic (for western Europe chronologies) and temperate (for central Europe chronologies) types. These two groups originated as the result of constraining the maximum distance among sites at the group level to 1,000 km (i.e., the spatial range of coherent tree-ring signals as inferred from correlograms). Therefore, five different groups were defined. Each group consisted of a number of neighbouring forest stands (≥3) that ensured a solution to mixed model estimates.

A number of variance-covariance (VCOV) models accommodating between- and within-group variability were tested and compared using Akaike and Bayesian information criteria for model selection, which favour parsimonious models (Burnham & Anderson, 2002). The VCOV models were broad evaluation (denoting common synchrony across groups), narrow evaluation (corresponding to a banded main diagonal matrix denoting perfect asynchrony between groups), unstructured (a completely general covariance matrix), compound symmetry (a matrix having constant variance and covariance) and variants of a Toeplitz structure (a matrix allowing for different (co)variances depending on the relative proximity or neighbourhood among groups). These models are described in detail in Table S2. Afterwards, estimates of growth synchrony ($\hat{a}$) were derived using the best VCOV model for the entire period (1901–2003) (Shestakova et al., 2018). The evolution of changes in $\hat{a}$ was also studied for successive 50-year segments lagged one year by fitting the same VCOV models.

The best fitting model was independently selected for each segment. This was done to characterise shifts in common $TRW_i$ variability over time potentially related to instability in the relationship between tree growth and climate factors at the high-frequency domain. Significant trends were determined by using the non-parametric Kendall $\tau$ rank correlation coefficient.

Relationships between radial growth and carbon isotope discrimination

The temporal (yearly) association between $TRW_i$ and $\Delta^{13}C_i$ (hereafter, $r_Y$) was investigated at the group level through a bivariate mixed-effects model (Appendix 3.2) (Shestakova et al., 2017). Broadly speaking, this approach estimates the extent by which $TRW_i$ and $\Delta^{13}C_i$, measured on the same set of chronologies, contain overlapping information as a result of plant processes related to carbon uptake and water use. Hence, the relevance of a physiological attribute ($\Delta^{13}C_i$) as determinant of regional forest growth is quantified by estimating how much of $TRW_i$ variability across chronologies is associated with the variability of isotopic records. We argue that this quantification is relevant for studying the variable role of a putative physiological tracer of productivity across large areas. The bivariate analysis was performed for the entire period (1901–2003). We also evaluated the changes in $r_Y$ between $TRW_i$ and $\Delta^{13}C_i$ chronologies for successive 50-year segments lagged one year.

*Meteorological data*

Monthly mean temperature, precipitation and potential evapotranspiration were used for climate characterization. Meteorological variables were obtained from the nearest grid point to each site of the high-resolution climate dataset (Climatic Research Unit, CRU TS 3.21; Harris, Jones, Osborn, & Lister, 2014). CRU provides climate series on a 0.5° × 0.5° grid-box basis, interpolated from meteorological stations across the globe, and extends back to 1901. However, it should be noted that climate data mainly originate from low-elevation stations. This leads to remarkable differences in elevation between stations and sampling sites in mountainous Mediterranean areas. To account for this discrepancy, we applied lapse rate adjustments to the CRU dataset for the Mediterranean sites (<45°N) following Gandullo (1994). Potential evapotranspiration was estimated from CRU records using the Hargreaves method (Hargreaves & Samani, 1982).

Bootstrapped correlations between $TRW_i$ or $\Delta^{13}C_i$ chronologies and monthly temperature, precipitation and the Standardized Precipitation-Evapotranspiration Index (SPEI3, a 3-month integrated drought index; Vicente-Serrano, Beguería, & López-Moreno, 2010) were

computed over the period 1901–2003 to examine site-specific responses to climate. To assess the temporal stability of these responses, the same analysis was conducted for the split 1901–1950 and 1951–2003 periods. To ensure that results were driven by local climate rather than by long-term trends (e.g., global warming), the climatic series exhibiting a linear trend over time were detrended by fitting a straight line and keeping the residuals of these linear fits or, otherwise, simply differencing from the mean. Climate relationships were analysed from the previous October to the current September of tree-ring formation.

*Analysis of biogeographical patterns of tree performance*

To characterize the spatial patterns of tree growth and its dependence on $\Delta^{13}C$, changes in growth synchrony ($\hat{a}$) and in the relationship between $TRW_i$ and $\Delta^{13}C_i$ ($r_Y$) were evaluated as a function of biophysical variables through simple correlations. We used geographic (latitude, longitude and elevation) and climatic records (mean annual temperature [MAT], mean annual precipitation [MAP] and potential evapotranspiration [PET]; period 1901–2003) averaged across sites for every group. It should be noted that climatic records in the network strongly depended on geographic location: MAT decreased linearly with increasing latitude ($r = –0.61$, $P < 0.01$) and longitude (or distance inland from the Atlantic Sea) ($r = –0.50$, $P < 0.05$), but it was not related to elevation. Similarly, PET was negatively related to latitude ($r = –0.84$, $P < 0.001$) and longitude ($r = –0.58$, $P < 0.01$), and positively to elevation ($r = 0.45$, $P < 0.05$). MAP was also positively related to elevation ($r = 0.45$, $P < 0.05$). The stability of these relationships was assessed through correlation analysis for the split 1901–1950 and 1951–2003 periods.

**Results**

*Site-level growth trends and responses to climate*

Eleven sites showed positive BAI trends and one site showed a negative BAI trend (slope *b*, $P < 0.05$) for the period 1901–2003, while no significant trend was detected for seven sites (Table 1). Growth acceleration was observed at all oak sites and at three pine sites from mid and high latitudes, whereas growth significantly declined in a Mediterranean site. High summer temperatures enhanced growth in Fennoscandia, whereas summer drought often constrained growth at central and southern latitudes (as indicated by negative correlations with summer temperature and positive correlations with summer precipitation and SPEI3) (Fig. S1a–c). In addition, the positive growth responses to high winter temperatures observed at some mid- and low-latitude sites suggested co-limitation by cold winters and dry summers. In comparison,

more clear-cut climate signals were shared by $\Delta^{13}C_i$ records, which were especially associated with summer temperatures (negatively) and summer precipitation and SPEI3 (positively) (Fig. S1d–f).

*Spatial consistency of tree-ring signals*

Naturally, the correlations between pairs of chronologies for $TRW_i$ decreased with increasing distance between sites. This effect accounted for 29% variability of inter-site correlation coefficients if subject to exponential decay (Fig. 1a). The highest correlations were found between *Quercus* stands from central Europe and between *Pinus* stands from north-eastern Europe ($r \geq 0.30$). Significant spatial autocorrelation was recorded up to 1,000 km, with a mean correlation of 0.22 and 0.12 for sites within distances of 0–500 and 501–1,000 km, respectively (Fig. 1c). A Principal Component Analysis performed on $TRW_i$ returned five principal components (PCs) that accounted for 50% of the total variance. The first PC, which explained 12.9% of variance, had positive loadings for all chronologies, except for one Iberian site with *P. sylvestris* and the Moroccan site with *C. atlantica* (Fig. S2). The highest PC1 loadings corresponded to western and central European chronologies, indicating larger growth similarities compared to peripheral chronologies, located farther away from each other. The second PC, which explained 11.0% of variance, was also related to the geographic location of chronologies: positive PC2 loadings corresponded to south-western chronologies, while north-eastern chronologies had negative loadings (Fig. S2). The remaining three PCs accounted for <10% of variance and showed mixed spatial signals, indicating species-specific differences and the influence of local conditions on tree growth.

For $\Delta^{13}C_i$ chronologies, we found an exponential decrease in coherence with distance between chronology pairs accounting for 28% variability of inter-site correlation coefficients (Fig. 1b). Significant spatial autocorrelations were recorded up to 1,000 km (Fig. 1d). Similarly, the analysis of spatial autocorrelation in climate parameters revealed that the common signal declined with distance (Fig. S3a,b) and extended >2,500 km for MAT (linear function) and up to 1,000 km for MAP (decay function) (Fig. S3c,d). There was also a significant negative association between the most distant sites (>2,500 km) for MAP.

*Tree growth synchrony across Europe*

The five climate groups identified across the network consisted of three to five chronologies sharing temporal growth patterns (Fig. 2). A heterogeneous Toeplitz with two bands was the best model for the period 1901–2003, indicating covariation between neighbouring groups only

(Table S3). Growth synchrony ($\hat{a}$) varied considerably among groups, ranging from 0.06 ± 0.01 (Mediterranean) to 0.36 ± 0.06 (Boreal) (mean ± SE) (Fig. 3a). The $\hat{a}$ values were unrelated to the average distance between sites at the group level, with groups showing the lowest and highest $\hat{a}$ having inter-site distances of 785 ± 118 km and 913 ± 119 km (mean ± SE), respectively. In addition, the variable number of chronologies at the group level did not influence $\hat{a}$. At the between-group level, the highest $\hat{a}$ was found between Boreal and cold continental forests (0.11 ± 0.02), with progressively decreasing common signals between neighbours observed southwards (Fig. 3b).

Differences in synchrony among groups were geographically structured and related to latitude ($r = 0.96$, $P < 0.01$) and longitude ($r = 0.89$, $P < 0.05$), but not to elevation (Fig. S4). At the site level, however, there were strong associations between latitude and longitude ($r = 0.65$, $P < 0.01$), latitude and elevation ($r = –0.59$, $P < 0.01$), and longitude and elevation ($r = –0.44$, $P < 0.10$). To check for geographic consistency in these synchrony gradients across Europe, we examined an independent, larger dataset of ring-width chronologies obtained from the International Tree-Ring Data Bank (Grissino-Mayer & Fritts, 1997) having the same species representation ($n = 80$; 52 *Pinus* chronologies and 28 *Quercus* chronologies) (Appendix 4). In this case, we also detected a strong latitudinal gradient in $\hat{a}$ (Fig. S5). Consequently, we assumed that this trend was essentially independent of the particular tree-ring network under consideration. The observed geographic gradient in growth synchrony was also analysed in relation to the potential climatic drivers of forest performance across Europe. Notably, climate variables explained most geographic variation in $\hat{a}$ among groups (Fig. S6). We found strong negative relationships between $\hat{a}$ and PET, followed by MAP and MAT, which are consistent with a gradual decrease in evapotranspirative demand and temperature with increasing latitude.

*Temporal changes in growth synchrony*

The synchrony patterns changed markedly across Europe over the 20$^{th}$ century. $\hat{a}$ increased at low and mid latitudes (i.e., in Atlantic, Mediterranean and temperate forests), whereas it decreased at high latitudes (especially in Boreal, but also in cold continental forests) (Fig. 4a). Such divergent geographic trends weakened the relation between $\hat{a}$ and biogeographic factors, resulting in less geographically- and climatically-dependent $\hat{a}$ values across the continent after 1950 (Fig. S4, S6). At the between-group level, different trends were observed depending on the particular group combination. For neighbouring groups, we found a substantial decrease in synchrony between Boreal and cold continental forests, whereas synchrony remained steady or increased for other group combinations (Fig. 4b). A modest, albeit sizeable common signal

emerged among the more geographically distant group pairs after 1960 ($\hat{a} \approx 0.05$-$0.10$) (Fig. 4c). In fact, synchrony among forest types strongly converged across Europe in the second half of the century. In contrast, we did not find changes in synchrony patterns of climate parameters (MAT, MAP) throughout the 20$^{th}$ century (results not shown). This led us to discard the possibility that the observed changes in growth synchrony had been driven by concomitant fluctuations in synchrony of climate factors.

*Tree growth patterns as related to isotopic signals*

The temporal variability shared by $TRW_i$ and $\Delta^{13}C_i$ ($r_Y$) was investigated at the group level. We found very different, geographically-structured relationships between these traits. The association was mainly positive (for Atlantic, cold-continental and temperate forests) or very positive (for Mediterranean forests), being significantly negative for Boreal forests (Fig. 5), hence following a latitudinal gradient ($r = –0.96$, $P < 0.05$) (Fig. S7). Conversely, $r_Y$ was non-significant for neither longitude nor elevation (Fig. S7). In addition, $r_Y$ was correlated to climate variables at the group level, with the strongest positive association found for both PET and MAP (Fig. S8).

The association between $TRW_i$ and $\Delta^{13}C_i$ changed markedly across Europe throughout the 20$^{th}$ century. $r_Y$ turned from negative to non-significant in Boreal forests, and changed from non-significant to positive in cold-continental (recently), temperate and Mediterranean forests (Fig. 6). As a result, $TRW_i$ and $\Delta^{13}C_i$ mainly became positively related across Europe. The latitudinal pattern of $r_Y$ was also stronger in the second than in the first half of the century (Fig. S7). This relationship became more dependent on PET after 1950 (Fig. S8).

## Discussion

This study yields evidence for geographically-structured patterns of forest growth and its associations with carbon isotope fractionation processes across Europe. Common tree growth and physiology were shared by stands spread up to 1,000 km. This outcome provides a general indication on the geographical extent by which climate factors influence tree performance continent-wide; indeed, no other environmental driver is likely to act on the same spatial scale at the high-frequency domain (Fritts, 2001).

*Geographic structure and climatic controls of tree-ring signals in European forests*

Differential growth responses to climate were evident across the network, with temperature-sensitive growth at northern latitudes, precipitation-sensitive growth at central-southern

latitudes, and mixed signals in temperate and high-elevation European forests (Babst et al., 2013). Conversely, the extent of common climate signals present in carbon isotopes suggests a tight stomatal control of water losses and, indirectly, photosynthetic activity during summer across most of Europe (Cullen, Adams, Anderson, & Grierson, 2008). These results suggest a partial de-coupling between leaf- and stem-level processes (Jucker et al., 2017). They are consistent with current evidence supporting that carbon allocation patterns change with increasing temperature and this change varies between tree species from different biomes and functional groups (Way & Oren, 2010). Details on the nature and magnitude of carbon isotope signals across the network have been reported by Treydte et al. (2007).

*Interpreting ring-width patterns continent-wide*

Our results show a marked geographical organization of 20$^{th}$-century growth patterns across Europe. The most conspicuous changes in synchronous tree growth occurred along a north–south gradient, with $\hat{a}$ increasing northwards concurrent with a thermal gradient of decreasing temperature and reduced evapotranspiration (Babst et al., 2013). This agrees with our hypothesis of more synchronous growth in cold-limited, high-latitude forests owing to the greater spatial homogeneity of temperature effects on tree growth in northern Europe (Düthorn, Schneider, Günther, Gläser, & Esper, 2016). It contrasts with the more geographically complex drought events occurring in central and southern Europe (Orlowsky & Seneviratne, 2014), hence resulting in substantially less synchronous growth patterns (Shestakova et al., 2016).

Notably, $\hat{a}$ increased after 1950 except in Fennoscandia, which weakened the northward trend of enhanced synchrony observed during the preceding period. This outcome suggests warming-induced climatic forcing spreading across central and southern Europe, irrespective of species and local site conditions, thus enhancing synchrony through common tree sensitivity to such emergent exogenous factor (Fig. S9). It is in line with previous findings on recent high-frequency adjustments of ring-width patterns in response to amplified drought effects on growth in temperate and semiarid regions (Latte, Lebourgeois, & Claessens, 2015; Shestakova et al., 2016). In contrast, climate warming would progressively mitigate low-temperature constraints on tree performance occurring in Boreal forests (Düthorn et al., 2016). This leads to an increasing importance of local (stand-level) effects on tree growth over time, hence triggering regional asynchrony (but see Shestakova et al., 2016). We interpret these phenomena as a sign of increasing drought effects on forest growth dynamics expanding northwards across Europe, which are concurrent with temperature trends across the study area (+0.15 to +0.35°C decade$^{-1}$ between 1960 and 2015) (EEA, 2016).

*Carbon isotope fractionation relates to spatial patterns of forest growth in Europe*

We investigated the physiological mechanisms underlying geographically-structured temporal growth variability through bivariate random-effects modelling of the common temporal signal present in $TRW_i$ and $\Delta^{13}C_i$. This approach is appropriate for investigating exogenous constraints on forest growth and physiology acting over large (continental) climate gradients, because site-level impacts on tree-ring traits (e.g., differential management, competition, soil depth and fertility, etc.) are set aside explicitly from the analysis.

The positive relationships between $TRW_i$ and $\Delta^{13}C_i$ at low and mid latitudes suggest that stomatal limitation of leaf carbon assimilation is a key mechanism controlling tree growth synchrony south of 50°N in Europe (Fig. 5). Therefore, leaf-level physiology and tree growth are driven, to a relevant extent, by water stress at about half of the study area (including e.g., France, Austria and south of Germany and Poland) during the 20$^{th}$ century. Conversely, the negative relationship between $TRW_i$ and $\Delta^{13}C_i$ in Fennoscandia indicates that photosynthesis was constrained by low temperatures/sunshine hours (Gagen et al., 2011). At cool, moist sites the main control over water-use efficiency is assimilation rate, which can be limited by either enzyme activity (photon flux) or enzyme production (leaf temperature or nitrogen availability). These limitations would increase $\Delta^{13}C$ at the expense of decreased carbon uptake, hence reducing radial growth. Although our results must be weighed against the limited spatial representativeness of the sampling network, they allow delineating broad geographical trends that so far have been difficult to ascertain continent-wide, partly due to the unsystematic and sparse nature of data collection (Saurer et al., 2014). Besides, the observed trends agree with previous studies performed across smaller areas showing strong positive ring-width *vs.* $\Delta^{13}C$ correlations for trees growing under water-limited conditions, but weak correlations at wetter and colder sites (Voelker et al., 2014; del Castillo, Voltas, & Ferrio, 2015).

*Strengthening of $\Delta^{13}C$–growth relationships in response to climate change*

The geographical structure of tree growth relationships with carbon isotope fractionation processes varied during the 20$^{th}$ century. Alongside the increase in growth synchrony observed at the temperate, cold-continental and Mediterranean groups, a change from non-significant to positive correlations suggests intensified drought impacts on tree physiology since 1950 (Saurer et al., 2014). Such warming-induced drought effects influencing stomatal regulation have been shown insufficient to decrease 20$^{th}$-century transpiration, as alternative factors (e.g., lengthened growing seasons or increased leaf area) counterbalance the impacts of leaf-level gas exchange

processes on whole-tree physiology (Frank et al., 2015). Indeed, we found evidence of growth enhancement across Europe, but mainly in oaks originating from moist temperate climates in low-elevation stands. For conifers, growth stimulation was observed in some of the cold-limited sites, while growth decline was found in drought-constrained Mediterranean mountains. In high-latitude and high-elevation sites, the increasing growth trend could be produced by a raise in photosynthetic rates, which is likely driven by a combination of rising $CO_2$, temperature and surface radiation. However, drought stress seems to override a positive effect of enhanced leaf intercellular $CO_2$ concentration in the Mediterranean region, resulting in no change or decline in productivity (Andreu-Hayles et al., 2011).

In Fennoscandia, the negative ring-width dependence on $\Delta^{13}C$ vanished after 1950, which suggests that an earlier photosynthetic limitation of growth driven by low temperatures, high cloudiness or both factors has attenuated in recent decades. In the western Mediterranean, this dependence changed abruptly from zero to nearly one after 1970. Previously, growth synchrony among the group chronologies was absent, rendering a null signal shared by ring-width and $\Delta^{13}C$. After 1950, a common growth signal was low but relevant: this signal was essentially related to $\Delta^{13}C$ fluctuations, resulting in a highly positive correlation. Although this correlation implies a tight stomatal control of common radial growth in high-mountain Mediterranean forests, the limited number of chronologies and the sudden change in tree performance between periods might question this interpretation. A recent study carried out in Iberian mountain forests allows the downscaling of our results to a local area (Shestakova et al., 2017). These authors reported that multispecies tree growth at about 1,500 m is more dependent on a tighter stomatal control of water losses (inferred from $\Delta^{13}C$) since the 1980s, hence resembling lower elevation stands. These results reinforce our view, although more data supporting this evidence are still needed on a regional scale. Unfortunately, studies on long-term shifts in radial growth related to switches of the main environmental limitations to photosynthetic carbon gain are still scarce (Voelker et al., 2014).

To conclude, we have reported forest shifts from temperature- to moisture-sensitive growth spreading northwards continent-wide and associated to latitudinal changes in tree dependence on carbon isotope fractionation processes. Leaf-level physiology and radial growth of trees are ultimately linked via carbon allocation strategies. Common signals imprinted in ring-width and stable isotopes have been broadly reported, either along geographical gradients (i.e., phenotypic plasticity; del Castillo et al., 2015), over time (i.e., temporal covariation; Voelker et al., 2014; Shestakova et al., 2017; this work) or at the intraspecific level (i.e., genetic correlation; Fardusi et al., 2016). These evidences support (direct or indirect) effects of carbon

uptake processes on above-ground growth. On the other hand, carbohydrates are used for various other processes than growth (e.g., maintenance, respiration, reproduction) and carbon availability is seldom considered to limit tree growth (Palacio, Hoch, Sala, Körner, & Millard, 2014; but see Wiley & Helliker, 2012), which suggests that the relationship between productivity and stable isotopes may not be straightforward (Jucker et al., 2017). Alternative physiological mechanisms related to above-ground growth may interact with photosynthetic processes; for example, a critical turgor disrupting cell growth or the appearance of hydraulic constraints under drought (Sperry, 2000), or the weakening of meristematic growth under low temperatures (Rossi et al., 2016). These mechanisms would need to be carefully assessed against stable isotope signals.

Together with climate change, the increasing $_{atm}CO_2$ may have played a role in the observed shift in growth synchrony and the stronger relation between $\Delta^{13}C$ and $TRW_i$. Disentangling the relative effects of climate and $CO_2$ fertilization on spatially structured tree-ring information is challenging because both low- and high-frequency signals overlap impacting on tree physiology, carbon allocation and above- and below-ground growth. Additional factors interacting with climate change and $_{atm}CO_2$ such as increasing nutrient limitations (Jonard et al., 2015) or atmospheric deposition (de Vries, Dobbertin, Solberg, van Dobben, & Schaub, 2014) should also be considered. A previous study on the same tree-ring network demonstrated that $CO_2$ fertilization has increased water-use efficiency of European forests in the 20$^{th}$ century (Saurer et al., 2014). However, these increments were not spatially uniform and, notably, the strongest increase was reported in response to summer drought for temperate forests in central Europe, an area in which we observe large increases in growth synchrony. These findings definitely point to an increasing impact of water stress spreading northwards across European forests. Therefore, this research demonstrates that broad-scale climatic variation jointly influences tree ecophysiology and productivity in previously unrecognized ways, and sheds more light on the ecological implications of ecosystem functioning under the new climate conditions.

## References


Anderegg, W. R. L., Klein, T., Barlett, M., Sack, L., Pellegrini, A.F., Choat, B., & Jansen, S. (2016). Meta-analysis reveals that hydraulic traits explain cross-species patterns of drought-induced tree mortality across the globe. *Proceedings of the National Academy of Sciences of the United States of America*, **113**, 5024–5029.

Andreu-Hayles, L., Gutiérrez, E., Muntan, E., Helle, G., Anchukaitis, K. J., & Schleser, G. H. (2011). Long tree-ring chronologies reveal 20$^{th}$ century increases in water-use efficiency but no enhancement of tree growth at five Iberian pine forests. *Global Change Biology*, **17**, 2095–2112.

Babst, F., Poulter, B., Trouet, V., Tan, K., Neuwirth, B., Wilson, R., Carrer, M., Grabner, M., Tegel, W., Levanič, T., Panayotov, M., Urbinati, C., Bouriaud, O., Ciais, P., & Frank, D. (2013). Site- and species-specific responses of forest growth to climate across the European continent. *Global Ecology and Biogeography*, **22**, 706–717.

Burnham, K.P., & Anderson, D.R. (2002) *Model selection and multi-model inference: A practical information – theoretic approach*. Springer, New York 488 pp.

Cernusak, L. A., & English, N. B. (2015). Beyond tree-ring widths: stable isotopes sharpen the focus of climate response of temperate forest trees. *Tree Physiology*, **35**, 1–3.

Chown, S. L., Gaston, K. J., & Robinson, D. (2004). Macrophysiology: large-scale patterns in physiological traits and their ecological implications. *Functional Ecology*, **18**, 159–167.

Cook, E. R., & Kairiukstis, L. A. (1990). *Methods of dendrochronology: Applications in the environmental sciences*. Dordrecht, Netherlands: Springer Netherlands.

Cullen, L. E., Adams, M. A., Anderson, M. J., & Grierson, P. F. (2008). Analyses of $\delta^{13}C$ and $\delta^{18}O$ in tree rings of *Callitris columellaris* provide evidence of a change in stomatal control of photosynthesis in response to regional changes in climate. *Tree Physiology*, **28**, 1525–1533.

de Vries, W., Dobbertin, M. H., Solberg, H., van Dobben, H. F., & Schaub, M. (2014). Impacts of acid deposition, ozone exposure and weather conditions on forest ecosystems in Europe: an overview. *Plant and Soil*, **380**, 1–45.

del Castillo, J., Voltas, J., & Ferrio, J. P. (2015). Carbon isotope discrimination, radial growth, and NDVI share spatiotemporal responses to precipitation in Aleppo pine. *Trees*, **29**, 223–233.

Düthorn, E., Schneider, L., Günther, B., Gläser, S., & Esper, J. (2016). Ecological and climatological signals in tree-ring width and density chronologies along a latitudinal boreal transect. *Scandinavian Journal of Forest Research*, **31**, 750–757.

591 European Environment Agency (2016). *Trends in annual temperature across Europe between*
592 *1960 and 2015*. [WWW document] URL http://www.eea.europa.eu/data-and-
593 maps/figures/decadal-average-trends-in-mean-6. [accessed 1 August 2018].
594 Fardusi, M. S., Ferrio, J. P., Comas, C., Voltas, J., Resco de Dios, V., & Serrano, L. (2016).
595 Intra-specific association between carbon isotope composition and productivity in
596 woody plants: a meta-analysis. *Plant Science*, **251**, 110–118.
597 Farquhar, G. D., Ehleringer, J. R., & Hubick, K. T. (1989). Carbon isotope discrimination and
598 photosynthesis. *Annual Review of Plant Physiology and Plant Molecular Biology*, **40**,
599 503–537.
600 Frank, D. C., Poulter, B., Saurer, M., Esper, J., Huntingford, C., Helle, G., Treydte, K.,
601 Zimmermann, N. E., Schleser, G. H., Ahlström, A., Ciais, P., Friedlingstein, P., Levis,
602 S., Lomas, M., Sitch, S., Viovy, N., Andreu-Hayles, L., Bednarz, Z., Berninger, F.,
603 Boettger, T., D'Alessandro, C. M., Daux, V., Filot, M., Grabner, M., Gutierrez, E.,
604 Haupt, M., Hilasvuori, E., Jungner, H., Kalela-Brundin, M., Krapiec, M., Leuenberger,
605 M., Loader, N. J., Marah, H., Masson-Delmotte, V., Pazdur, A., Pawelczyk, S., Pierre,
606 M., Planells, O., Pukiene, R., Reynolds-Henne, C. E., Rinne, K. T., Saracino, A.,
607 Sonninen, E., Stievenard, M., Switsur, V. R., Szczepanek, M., Szychowska-Krapiec, E.,
608 Todaro, L., Waterhouse, J. S., & Weigl, M. (2015). Water-use efficiency and
609 transpiration across European forests during the Anthropocene. *Nature Climate Change*,
610 **5**, 579–584.
611 Fritts, H. C. (2001). *Tree rings and climate*. Caldwell, NJ: Blackburn Press.
612 Gagen, M., Zorita, E., McCarroll, D., Young, G. H. F., Grudd, H., Jalkanen, R., Loader, N. J.,
613 Robertson, I., & Kirchhefer, A. (2011). Cloud response to summer temperatures in
614 Fennoscandia over the last thousand years. *Geophysical Research Letters*, **38**, L05701.
615 Gandullo, J. M. (1994). *Climatología y ciencia del suelo*. Madrid, Spain: Fundación Conde del
616 Valle de Salazar.
617 Gessler, A., Ferrio, J. P., Hommel, R., Treydte, K., Werner, R., & Monson, R. K. (2014). Stable
618 isotopes in tree rings: toward a mechanistic understanding of fractionation and mixing
619 processes from the leaves to the wood. *Tree Physiology*, **34**, 796–818.
620 Gibert, A., Gray, E. F., Westoby, M., Wright, I. J., & Falster, D. S. (2016). On the link between
621 functional traits and growth rate: meta-analysis shows effects change with plant size, as
622 predicted. *Journal of Ecology*, **104**, 1488–1503.

Grissino-Mayer, H. D, & Fritts, H. C. (1997). The International Tree-Ring Data Bank: an enhanced global database serving the global scientific community. *Holocene*, **7**, 235–228.

Hamed, K. H., & Rao, A. R. (1998). A modified Mann Kendall trend test for autocorrelated data. *Journal of Hydrology*, **204**, 182–196.

Hargreaves, G. H., & Samani, Z.A. (1982). Estimating potential evapotranspiration. *Journal of the Irrigation & Drainage Division – ASCE*, **108**, 225–230.

Harris, I., Jones, P. D., Osborn, T. J., & Lister, D. H. (2014). Updated high-resolution grids of monthly climatic observations – the CRU TS3.10 Dataset. *International Journal of Climatology*, **34**, 623–642.

Hartl-Meier, C., Zang, C., Büntgen, U., Esper, J., Rothe, A., Göttlein, A., Dirnböck, T., & Treydte, K. (2015). Uniform climate sensitivity in tree-ring stable isotopes across species and sites in a mid-latitude temperate forest. *Tree Physiology*, **35**, 4–15.

Jonard, M., Fürst, A., Verstraeten, A., Thimonier, A., Timmermann, V., Potočić, N., Waldner, P., Benham, S., Hansen, K., Merilä, P., Ponette, Q., de la Cruz, A. C., Roskams, P., Nicolas, M., Croisé, L., Ingerslev, M., Matteucci, G., Decinti, B., Bascietto, M., & Rautio, P. (2015). Tree mineral nutrition is deteriorating in Europe. *Global Change Biology*, **21**, 418–430.

Jones, H. G. (1992). *Plants and microclimate*. Cambridge, England: Cambridge University Press.

Jucker, T., Grossiord, C., Bonal, D., Bouriaud, O., Gessler, A., & Coomes, D. A. (2017). Detecting the fingerprint of drought across Europe's forests: do carbon isotope ratios and stem growth rates tell similar stories? *Forest Ecosystems*, **4**, 24.

Köppen, W., & Geiger, R. (1936). Handbuch der klimatologie. Berlin, Germany: Gebrüder Bornträger.

Koenig, W. D., & Knops, J. M. H. (1998). Testing for spatial autocorrelation in ecological studies. *Ecography*, **21**, 423–429.

Kress, A., Young, G. H. F., Saurer, M., Loader, N. J., Siegwolf, R. T. W., & McCarroll, D. (2009). Stable isotope coherence in the earlywood and latewood of tree-line conifers. *Chemical Geology*, **268**, 52–57.

Latte, N., Lebourgeois, F., & Claessens, H. (2015). Increased tree-growth synchronization of beech (*Fagus sylvatica* L.) in response to climate change in northwestern Europe. *Dendrochronologia*, **33**, 69–77.

Livingston, N.J., Whitehead, D., Kelliher, F.M., Wang, Y.P., Grace, J.C., Walcroft, A.S., Byers, J.N., Mcseveny, T.M. & Millard, P. (1998) Nitrogen allocation and carbon isotope fractionation in relation to intercepted radiation and position in a young *Pinus radiata* D. Don tree. *Plant, Cell & Environment*, **21**, 795–803.

Nabuurs, G. J., Lindner, M., Verkerk, P. J., Gunia, K., Deda, P., Michalak, R., & Grassi, G. (2013). First signs of carbon sink saturation in European forest biomass. *Nature Climate Change*, **3**, 792–796.

Orlowsky, B., & Seneviratne, S. I. (2014). On the spatial representativeness of temporal dynamics at European weather stations. *International Journal of Climatology*, **34**, 3154–3160.

Palacio, S., Hoch, G., Sala, A., Körner, C., & Millard, P. (2014). Does carbon storage limit tree growth? *New Phytologist*, **201**, 1096–1100.

Pivovaroff, A. L., Pasquini, S. C., De Guzman, M. E., Alstad, K. P., Stemke, J. S., & Santiago, L. S. (2016). Multiple strategies for drought survival among woody plant species. *Functional Ecology*, **30**, 517–526.

Rossi, S., Anfodillo, T., Čufar, K., Cuny, H. E., Deslauriers, A., Fonti, P., Frank, D., Gričar, J., Gruber, A., Huang, J. G., Jyske, T., Kašpar, J., King, G., Krause, C., Liang, E., Mäkinen, H., Morin, H., Nöjd, P., Oberhuber, W., Prislan, P., Rathgeber, C. B., Saracino, A., Swidrak, I., & Treml, V. (2016). Pattern of xylem phenology in conifers of cold forest ecosystems at the Northern Hemisphere. *Global Change Biology*, **22**, 3804–3813.

Saurer, M., Spahni, R., Frank, D. C., Joos, F., Leuenberger, M., Loader, N. J., McCarroll, D., Gagen, M., Poulter, B., Siegwolf, R. T. W., Andreu-Hayles, L., Boettger, T., Dorado Liñán, I., Fairchild, I. J., Friedrich, M., Gutiérrez, E., Haupt, M., Hilasvuori, E., Heinrich, I., Helle, G., Grudd, H., Jalkanen, R., Levanič, T., Linderholm, H. W., Robertson, I., Sonninen, E., Treydte, K., Waterhouse, J. S., Woodley, E. J., Wynn, P. M., & Young, G. H. (2014). Spatial variability and temporal trends in water-use efficiency of European forest. *Global Change Biology*, **20**, 332–336.

Shestakova, T. A., Aguilera, M., Ferrio, J. P., Gutiérrez, E., & Voltas, J. (2014). Unravelling spatiotemporal tree-ring signals in Mediterranean oaks: a variance–covariance modelling approach of carbon and oxygen isotope ratios. *Tree Physiology*, **34**, 819–838.

Shestakova, T. A., Gutiérrez, E., Kirdyanov, A. V., Camarero, J. J., Génova, M., Knorre, A. A., Linares, J. C., Resco de Dios, V., Sánchez-Salguero, R., & Voltas, J. (2016). Forests synchronize their growth in contrasting Eurasian regions in response to climate

warming. *Proceedings of the National Academy of Sciences of the United States of America*, **113**, 662–667.

Shestakova, T. A., Camarero, J. J., Ferrio, J. P., Knorre, A. A., Gutiérrez, E., & Voltas, J. (2017). Increasing drought effects on five European pines modulate $\Delta^{13}C$-growth coupling along a Mediterranean altitudinal gradient. *Functional Ecology*, **31**, 1359–1370.

Shestakova, T. A., Gutiérrez, E., & Voltas, J. (2018). A roadmap to disentangling ecogeographical patterns of spatial synchrony in dendrosciences. *Trees*, **32**, 359–370.

Sperry, J. S. (2000). Hydraulic constraints on plant gas exchange. *Agricultural and Forest Meteorology*, **104**, 13–23.

Stuiver, M., & Braziunas, T. F. (1987). Tree cellulose $^{13}C/^{12}C$ isotope ratios and climatic change. *Nature*, **328**, 58–60.

Treydte, K., Frank, D. C., Esper, J., Andreu, L., Bednarz, Z., Berninger, F., Boettger, T., D'Alessandro, C. M., Etien, N., Filot, M., Grabner, M., Guillemin, M. T., Gutierrez, E., Haupt, M., Helle, G., Hilasvuori, E., Jungner, H., Kalela-Brundin, M., Krapiec, M., Leuenberger, M., Loader, N. J., Masson-Delmotte, V., Pazdur, A., Pawelczyk, S., Pierre, M., Planells, O., Pukiene, R., Reynolds-Henne, C. E., Rinne, K. T., Saracino, A., Saurer, M., Sonninen, E., Stievenard, M., Switsur, V. R., Szczepanek, M., Szychowska-Krapiec, E., Todaro, L., Waterhouse, J. S., Weigl, M., & Schleser, G. H. (2007). Signal strength and climate calibration of a European tree-ring isotope network. *Geophysical Research Letters*, **34**, L24302.

Vicente-Serrano, S. M., Beguería, S., & López-Moreno, J. I. (2010). A Multiscalar drought index sensitive to global warming: the Standardized Precipitation Evapotranspiration Index. *Journal of Climate*, **23**, 1696–1718.

Violle, C., Reich, P. B., Pacala, S. W., Enquist, B. J., & Kattge, J. (2014). The emergence and promise of functional biogeography. *Proceedings of the National Academy of Sciences of the United States of America*, **111**, 13690–13696.

Voelker, S. L., Meinzer, F. C., Lachenbruch, B., Brooks, J. R., & Guyette, R. P. (2014). Drivers of radial growth and carbon isotope discrimination of bur oak (*Quercus macrocarpa* Michx.) across continental gradients in precipitation, vapour pressure deficit and irradiance. *Plant, Cell and Environment*, **37**, 766–779.

Way, D. A., & Oren, R. (2010). Differential responses to changes in growth temperature between trees from different functional groups and biomes: a review and synthesis of data. *Tree Physiology*, **30**, 669–688.

Werner, C., Schnyder, H., Cuntz, M., Keitel, C., Zeeman, M. J., Dawson, T. E., Badeck, F. W., Brugnoli, E., Ghashghaie, J., Grams, T. E. E., Kayler, Z. E., Lakatos, M., Lee, X., Maguas, C., Ogee, J., Rascher, K. G., Siegwolf, R. T. W., Unger, S., Welker, J., Wingate, L., & Gessler, A. (2012). Progress and challenges in using stable isotopes to trace plant carbon and water relations across scales. *Biogeosciences*, **9**, 3083–3111.

Wiley, E. & Helliker, B. (2012). A re-evaluation of carbon storage in trees lends greater support for carbon limitation to growth. *New Physiologist*, **195**, 285-289.

**Data Accessibility Statement**

The tree-ring data used in this study are available upon request from the authors. Contact Emilia Gutiérrez (emgutierrez@ub.edu) for ring-width chronologies and Gerhard Helle (ghelle@gfz-potsdam.de) for carbon isotope records.

**Biosketch**

Tatiana A. Shestakova is a post-doctoral researcher at the Woods Hole Research Center, Falmouth, MA (USA). Her research interests include dendroecology, stable isotope biogeochemistry and climate change impacts on natural forest ecosystem. Particularly, she works on designing efficient inference tools and algorithms based on mixed modelling principles to understand the processes underlying the complexity and diversity in tree response patterns to environmental forcing and how these patterns are spatially structured across biogeographical gradients.

744 **FIGURE CAPTIONS**

745

746 Figure 1. Spatial patterns of indexed tree-ring traits across Europe for the period 1901–2003:
747 **(a, c)** indexed tree-ring width ($TRW_i$), **(b, d)** indexed carbon isotope discrimination ($\Delta^{13}C_i$).
748 *(Left panels)* Pairwise correlations of tree-ring chronologies as a function of geographical
749 distance. The patterns are summarized by regressing the correlation coefficients (*r* values)
750 involving pairs of chronologies (*y*-axis) on their corresponding distance (*x*-axis) by using
751 negative exponential functions ($y = be^{-cx}$). Different dot colors indicate pairwise correlations
752 within and between functional groups as follows: conifers (green), oaks (orange), and mixed
753 conifer–oak (blue). Asterisks after the coefficient of determination ($r^2$) indicate level of
754 significance ($^{***}P < 0.001$). *(Right panels)* Spatial structure of tree-ring traits across European
755 forests. The spatial autocorrelation in the tree-ring network was characterized for six
756 consecutive distance classes (listed on the *x*-axis). Mean *r* values and their statistical
757 significance (*P*) within each distance class were estimated from 1,000 randomizations.
758 Significant correlation coefficients ($P < 0.05$) are indicated by an asterisk.

759

760 Figure 2. Geographical distribution of sites, definition of groups of chronologies and synchrony
761 in radial growth at group level. Each dot identifies a chronology ($n \geq 20$ trees) according to the
762 codes shown in Table 1 (oak codes are shown in italics). Each colored encircled area identifies
763 a group of chronologies belonging to a particular climate type (see Table 1) that are separated
764 in pairs up to 1,000 km (see Fig. 1d for the distance threshold where significant radial growth
765 patterns are shared among chronologies). The corresponding growth synchrony at the group
766 level ($\hat{a}$) is shown within a rectangle. At least three neighbouring sites form a group (total
767 number of groups, $n = 5$). $\hat{a}$ values are estimated using indexed ring-width chronologies for the
768 period 1901–2003 as described in Appendix 3.1 (Supporting Information).

769

770 Figure 3. Growth synchrony across Europe. Patterns of growth synchrony ($\hat{a}$) at the within-
771 group level for the entire period 1901–2003 **(a)**. Patterns of growth synchrony ($\hat{a}$) at the
772 between-group level for the entire period 1901–2003 **(b)**. All calculations are based on indexed
773 ring-width chronologies. Groups sorted latitudinally from north to south. Error bars denote
774 standard errors.

775

776 Figure 4. Temporal trends in growth synchrony at within- and between-group levels for the
777 period 1901–2003. Growth synchrony ($\hat{a}$) is estimated for 50-year periods lagged by 5 year

following Eqs. 5 and 6 as described in Appendix 3.1 (Supporting Information). All calculations are based on indexed ring-width ($TRW_i$) chronologies. For the sake of visual clarity, the estimates of $\hat{a}$ are represented separately for pairs of chronologies belonging to the same group (i.e., within-group level) **(a)**, and for pairs of chronologies belonging to different groups (i.e., between-group level) for neighbouring **(b)** and non-neighbouring chronologies **(c)**. Grey lines denote the SE. Note the change in scale of the Y-axis between panels.

Figure 5. Geographical patterns of the relationship between $TRW_i$ and $\Delta^{13}C_i$ chronologies across Europe. The correlations at the group level ($r_Y$) are estimated for the entire period 1901–2003. Significant associations are depicted with an asterisk ($P < 0.10$). Error bars denote standard errors.

Figure 6. Temporal trends in associations between $TRW_i$ and $\Delta^{13}C_i$ chronologies at the group level for the period 1901–2003. The correlations ($r_Y$) are estimated for 50-year periods lagged by 5 year following Eq. 7 as described in Appendix 3.2 (Supporting Information). All calculations are based on indexed ring-width ($TRW_i$) and carbon isotope ($\Delta^{13}C_i$) chronologies. Grey lines denote the SE of $r_Y$. Significant correlations (correlation coefficients with 90% confidence intervals not embracing zero) are depicted as filled dots.

**Table 1**. Geographical features and climatic characteristics of the sampling sites. Sites are sorted latitudinally
Climate parameters were obtained based on CRU TS 3.21 data over the period 1901–2003. See Meteorologi
Methods for details. Climate types were estimated using the Köppen classification (Köppen & Geiger, 1936).

| No | Country | Site name | Code | Species | Latitude (°N) | Longitude (°E) | Elevation (m) | MAT (°C) | MAP (mm) | PET (mm) | MA |
|---|---|---|---|---|---|---|---|---|---|---|---|
| 1 | Finland | Kessi, Inari | INA | *Pinus sylvestris* | 68.93 | 28.42 | 150 | –1.2 | 432 | 413 | Ap |
| 2 | Finland | Sivak., Ilomantsi | ILO | *Pinus sylvestris* | 62.98 | 31.27 | 200 | 2.2 | 573 | 515 | Ap |
| 3 | Norway | Gutuli | GUT | *Pinus sylvestris* | 62.00 | 12.18 | 800 | 0.7 | 586 | 512 | Ap |
| 4 | Finland | Bromarv | BRO | *Quercus robur* | 60.00 | 23.08 | 5 | 4.9 | 568 | 562 | Ap |
| 5 | UK | Lochwood | LOC | *Quercus robur* | 55.27 | –3.43 | 175 | 7.4 | 1517 | 589 | |
| 6 | Lithuania | Panemunes Silas | PAN | *Pinus sylvestris* | 54.88 | 23.97 | 45 | 6.6 | 634 | 672 | A |
| 7 | Poland | Suwalki | SUW | *Pinus sylvestris* | 54.10 | 22.93 | 160 | 6.7 | 619 | 686 | A |
| 8 | UK | Woburn Abbey | WOB | *Quercus robur* | 51.98 | –0.59 | 50 | 9.5 | 709 | 724 | A |
| 9 | Germany | Dransfeld | DRA | *Quercus petraea* | 51.50 | 9.78 | 320 | 7.7 | 723 | 677 | A |
| 10 | UK | Windsor | WIN | *Pinus sylvestris* | 51.41 | –0.59 | 10 | 9.5 | 763 | 738 | A |
| 11 | Poland | Niepolomice, Gibiel | NIE1 | *Quercus robur* | 50.12 | 20.38 | 190 | 8.0 | 676 | 674 | Ap |
| 12 | Poland | Niepolomice, Gibiel | NIE2 | *Pinus sylvestris* | 50.12 | 20.38 | 190 | 8.0 | 676 | 674 | Ap |
| 13 | France | Fontainebleau | FON | *Quercus petraea* | 48.38 | 2.67 | 100 | 11.5 | 608 | 861 | M |
| 14 | France | Rennes | REN | *Quercus robur* | 48.25 | –1.70 | 100 | 11.1 | 733 | 786 | A |
| 15 | Austria | Lainzer Tiergarte | LAI | *Quercus petraea* | 48.18 | 16.20 | 300 | 9.6 | 654 | 792 | M |
| 16 | Austria | Poellau | POE | *Pinus nigra* | 47.95 | 16.06 | 500 | 8.3 | 815 | 762 | Ap |
| 17 | Spain | Pinar de Lillo | LIL | *Pinus sylvestris* | 43.07 | –5.25 | 1600 | 5.1 | 1505 | 688 | Ju |
| 28 | Spain | Massis de Pedraforca | PED | *Pinus uncinata* | 42.23 | 1.70 | 2100 | 3.9 | 1299 | 692 | Ju |
| 19 | Spain | Sierra de Cazorla | CAZ | *Pinus nigra* | 37.80 | –2.95 | 1816 | 8.9 | 712 | 1014 | M |
| 20 | Morocco | Col du Zad | COL | *Cedrus atlantica* | 32.97 | –5.07 | 2200 | 10.4 | 717 | 1163 | A |

Abbreviations: MAT, mean annual temperature; MAP, mean annual precipitation; PET, potential evapotranspiration; BAI, basal ar
$^{*}P < 0.05$; $^{**}P < 0.01$; $^{***}P < 0.001$. The significance of BAI trends is assessed using the Mann-Kendall non-parametric test which ac
autocorrelation (Hamed & Rao, 1998)

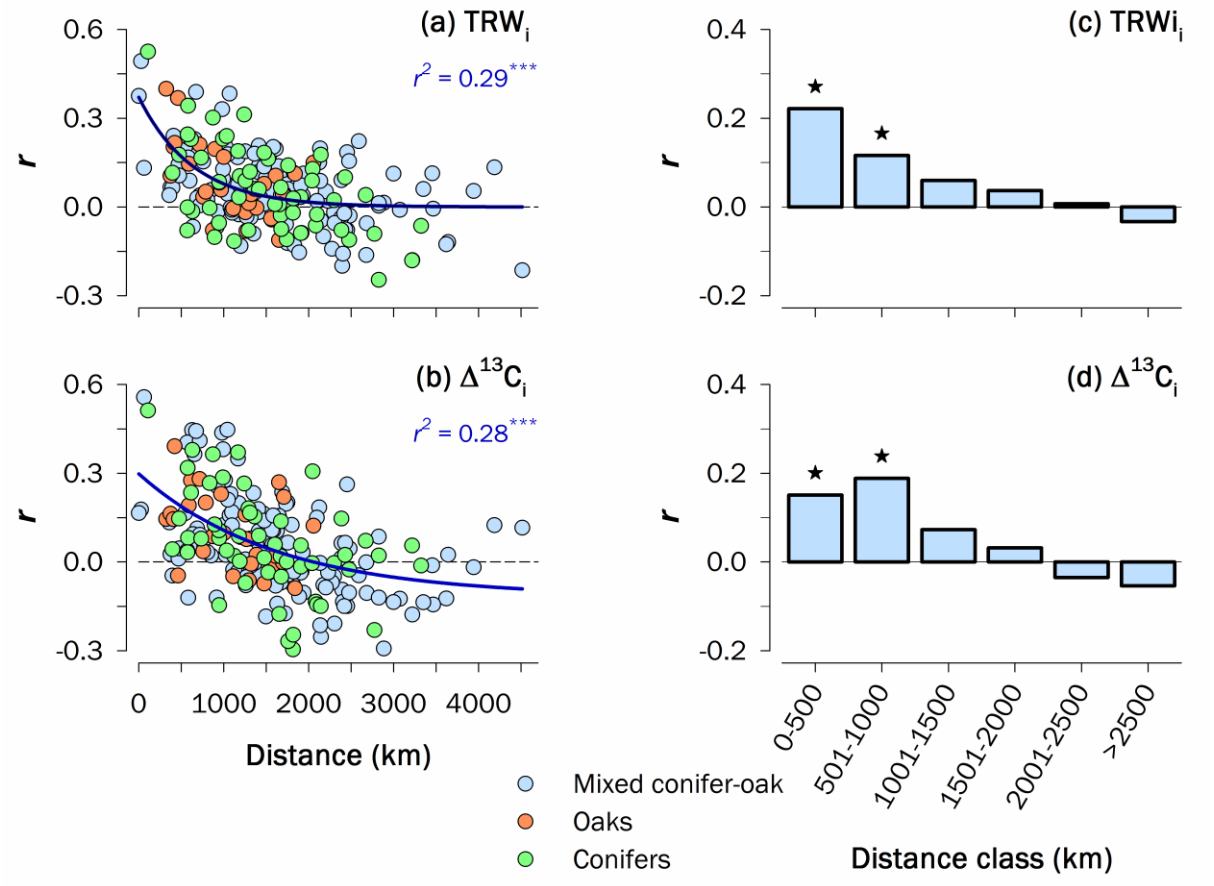
(a) TRW$_i$
$r^2$ = 0.29***
(b) Δ$^{13}$C$_i$
$r^2$ = 0.28***
r
Distance (km)
(c) TRWi$_i$
(d) Δ$^{13}$C$_i$
0-500
501-1000
1001-1500
1501-2000
2001-2500
>2500
Distance class (km)
Mixed conifer-oak
Oaks
Conifers

**Figure 1**

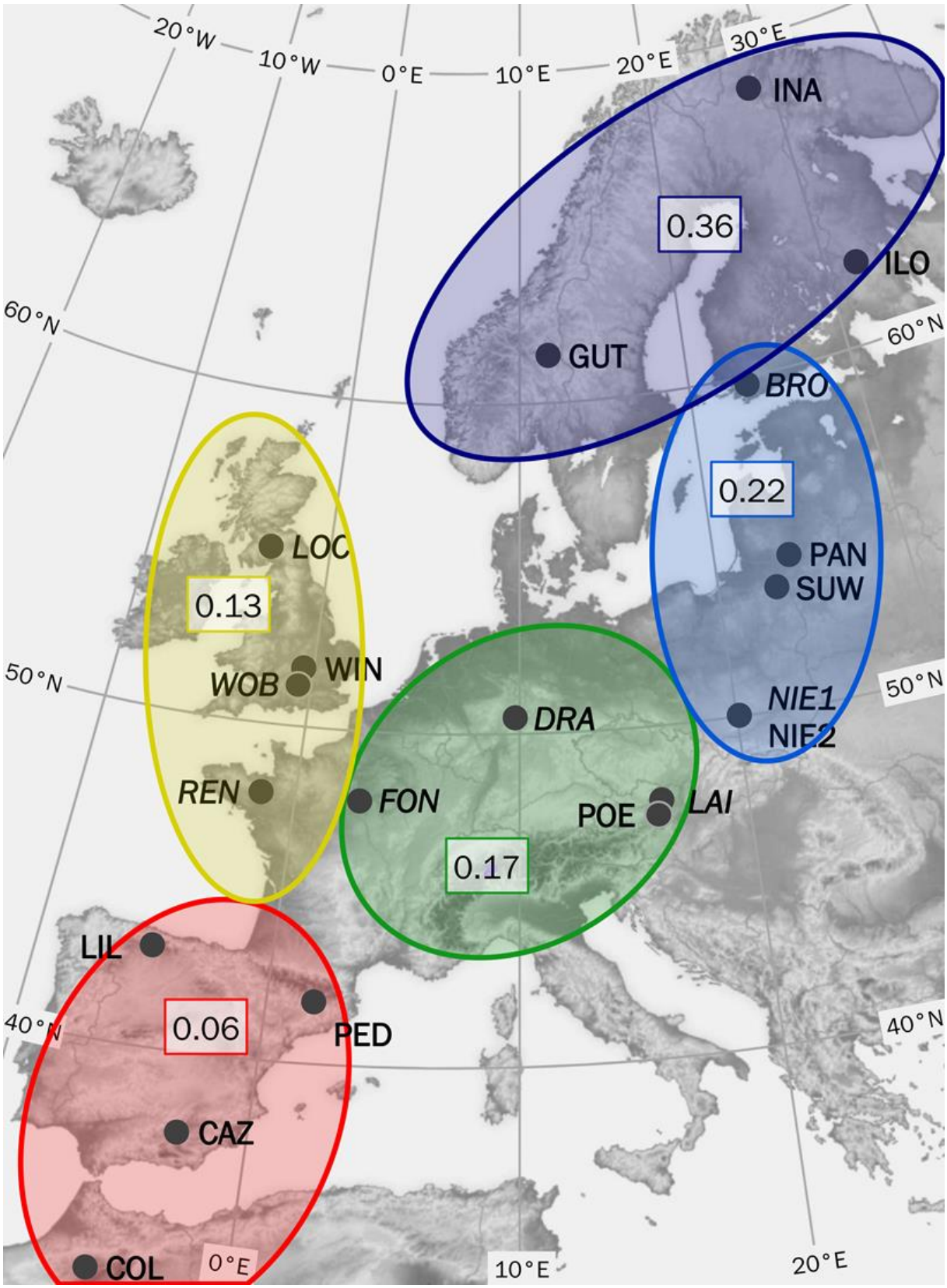
20°W
10°W
0°E
10°E
20°E
30°E
60°N
50°N
40°N
INA
0.36
ILO
GUT
BRO
0.22
PAN
SUW
LOC
0.13
WOB
WIN
NIE1
NIE2
DRA
REN
FON
POE
LAI
0.17
LIL
0.06
PED
CAZ
COL

**Figure 2**

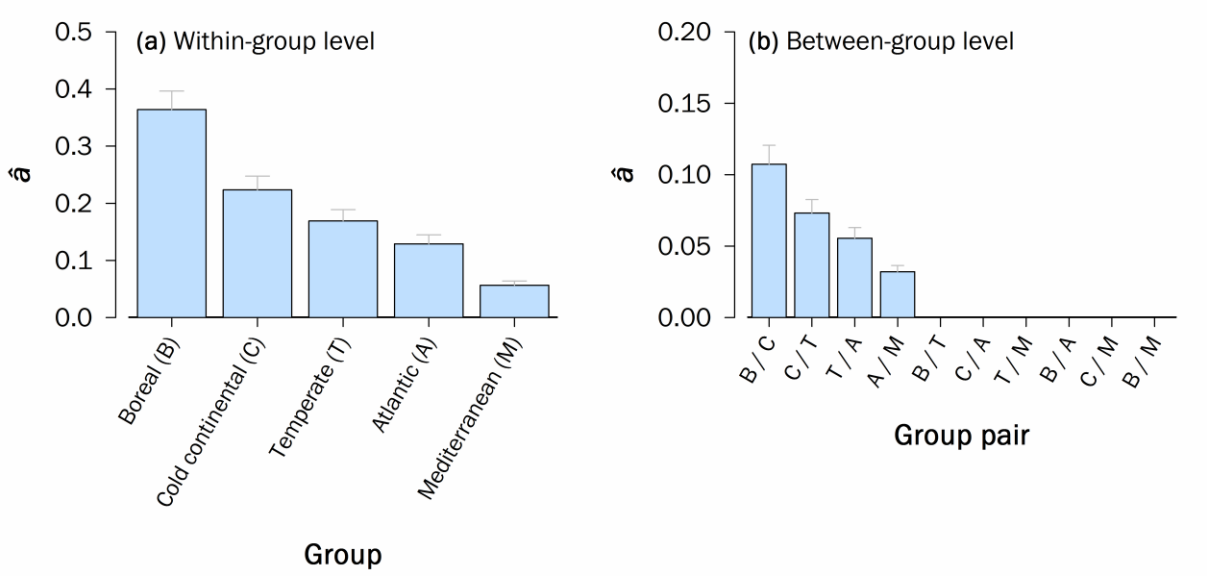


807

808 **Figure 3**

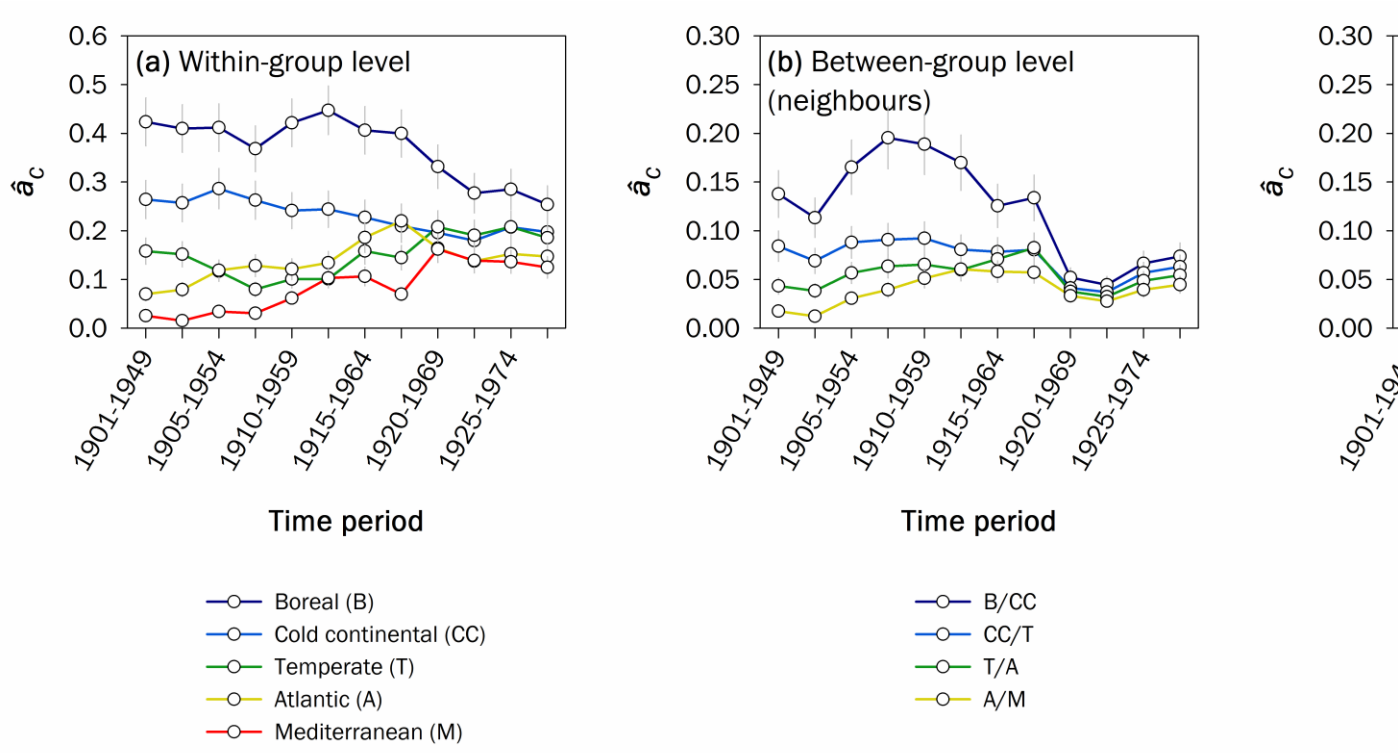


809

810 **Figure 4**

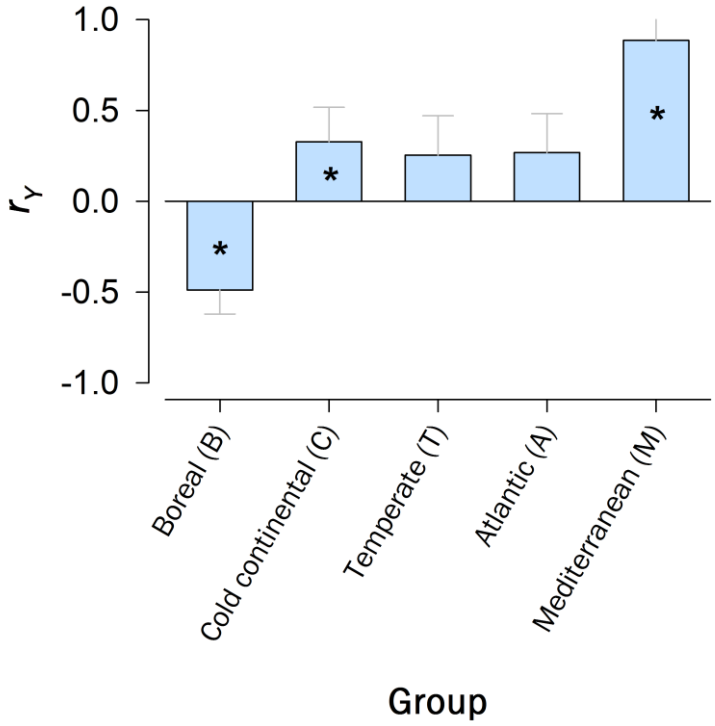


811

812 **Figure 5**

813

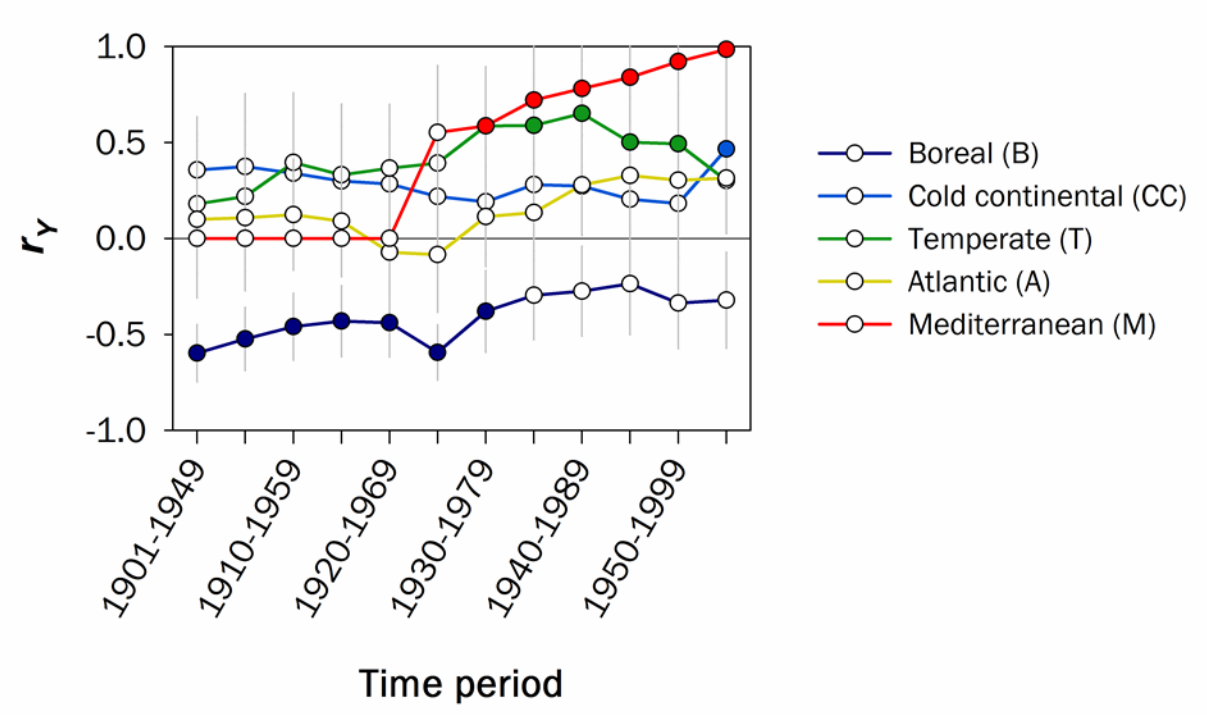
1.0
0.5
0.0
-0.5
-1.0
$r_Y$
1901-1949
1910-1959
1920-1969
1930-1979
1940-1989
1950-1999
Time period
Boreal (B)
Cold continental (CC)
Temperate (T)
Atlantic (A)
Mediterranean (M)

**Figure 6**

**Supporting Information**

Additional Supporting Information may be found in the online version of this article:

**Appendix 1**. Field sampling and tree-ring measurements.

**Appendix 2**. Tree-ring chronology characteristics.

**Appendix 3**. Random modelling analysis.

**Appendix 4**. Further evaluation of geographical trends in growth synchrony across Europe.

**Table S1**. Dendrochronological characteristics of the study sites.

**Table S2.** Description of variance-covariance (VCOV) models accommodating between- and within-group variability.

**Table S3.** Results of variance-covariance models for synchrony analysis.

**Figure S1**. Climate signals at the site level for $TRW_i$ and $\Delta^{13}C_i$ for the period 1901–2003.

**Figure S2**. Principal component analysis performed on 20 indexed ring-width chronologies distributed across Europe and northern Africa for the common period 1901–1998.

**Figure S3**.Spatial patterns of climate signals (mean annual temperature, MAT; mean annual precipitation, MAP) across Europe for the period 1901–2003.

**Figure S4**. Geographical patterns of growth synchrony ($\hat{a}$) at the group level for the entire period 1901–2003 and change in $\hat{a}$ for two consecutive periods (1901–1950 and 1951–2003).

**Figure S5**. Geographical patterns of growth synchrony ($\hat{a}$) for chronologies obtained from the International Tree-Ring Data Bank (ITRDB) dataset for the period 1901–2003.

**Figure S6.** Climatic patterns of growth synchrony ($\hat{a}$) at the group level for the entire period 1901–2003 and change in $\hat{a}$ for two consecutive periods (1901–1950 and 1951–2003).

**Figure S7**. Geographical patterns of the relationship between $TRW_i$ and $\Delta^{13}C_i$ chronologies across Europe for the entire period 1901–2003 and for two consecutive periods (1901–1950 and 1951–2003).

**Figure S8**. Climatic patterns of the relationship between $TRW_i$ and $\Delta^{13}C_i$ chronologies across Europe for the entire period 1901–2003 and for two consecutive periods (1901–1950 and 1951–2003).

**Figure S9**. Trends in climate parameters: mean annual temperature (MAT) and mean annual precipitation (MAP) at the group level.